THICK LIQUID FILM INSTABILITY MODEL USING CFD SIMULATIONS

Stanislav Knotek*, Miroslav Jícha*

The article presents a liquid film instability model designed using results of the set of CFD simulations. The governing equations of the model are derived using a linear equation of motion. The stability analysis is carried out by imposing a liquid surface disturbance which growth rate is investigated in dependence on the geometrical and physical configuration. The gas effect parameters, which are decisive variables in the model, are derived using results of the set of CFD simulations of turbulent flow in channel with wavy surface. The agreement between predicted and measured critical gas velocities and wavelengths in dependence on the liquid film thickness is very good.

Keywords : *liquid film, instability, waves, CFD*

1. Introduction

The liquid film sheared by gas flow in a horizontal enclosed channel has been broadly studied from half of twentieth century. From experimental studies published among others in [1], [2] and later for example in [3], it is well known that a number of different wave forms is generated on the liquid surface in dependence on the air velocity and the film thickness, eventually on the liquid flow rate. Using the measured data, so called wave regime map can be created such as is depicted in Fig. 1 using the experimental observations of Craik published in [2].
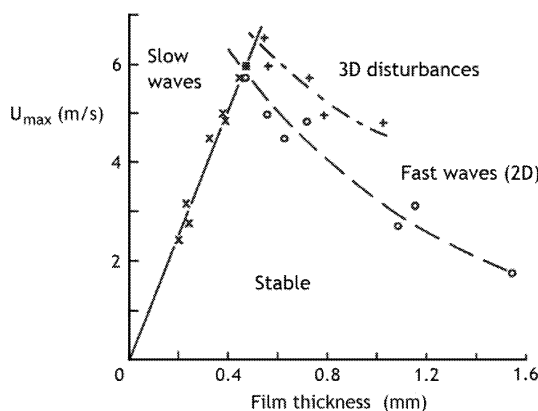

Fig.1: Maximum air velocity plotted against thickness of water film for the three transitions; taken from [2]

* Ing. S. Knotek, Ph.D., prof. Ing. M. Jícha, CSc., Brno University of Technology, Faculty of Mechanical Engineering, Energy Institute, Technická 2896/2, Brno

The figure shows that except the stable regime three wave types were observed. Typically, two or three dimensional waves cover the surface in dependence on the air velocity. However, for the liquid height lower than about $0.5\,\text{mm}$, so called slow waves appear. These long crested non-periodic waves define a third unstable regime which is generally observed for high air velocity and named solitary or capillary waves in dependence on the film thickness.

Given the various type of liquid film instabilities just mentioned, we have focused in this study only on the investigation of the conditions leading to the transition between the stable mode and two-dimensional waves on films with thickness larger than about $0.5\,\text{mm}$.

2. Methods

Simultaneously with the first experimental findings, the mathematical models of the initial instability as well as transitions between the wave regimes had been developed. The most used attitude is based on the linear analysis of the temporal growth of liquid surface fluctuations and the so called 'quasi-static' approximation which says that for large density and viscosity ratios between gas and liquid the wavy liquid surface can be considered as solid. Although there is uncertainty about how large these ratios must be, it is commonly assumed that the approximation is valid for air – water configuration.

2.1. Mathematical backgrounds of the linear analysis

The linear analysis of the liquid film instability is based on the Reynolds decompositions of the physical quantities into average and fluctuation parts. The liquid film displacement h' from its time averaged location $\bar{h}$ is defined in the form

$$h' = a \exp\{i\,\alpha\,(x - C\,t)\} = a \exp(\alpha\,C_\text{I}\,t) \exp\{i\,\alpha\,(x - C_\text{R}\,t)\}\ , \tag{1}$$

where a is the amplitude of the disturbance, x is the distance in the flow direction, $\alpha = 2\pi/\lambda$ is the wavenumber defined by the wavelength λ and $C = C_\text{R} + i\,C_\text{I}$ is the complex wave velocity. Given the formula (1), the interfacial disturbances are assumed as harmonic waves which propagate with phase velocity C_R and grow if $C_\text{I} > 0$. The most rapidly growing disturbance is the one for which $\alpha\,C_\text{I}$ is a maximum and the so called neutral stability condition $C_\text{I} = 0$ defines the desired transition from a stable to an unstable film.

The amplitude of the wave is assumed small enough that it induced a linear response in the velocity, shear stress and pressure field in the liquid. Thus, the wall shear stress and pressure fluctuations induced by a gas flow on the liquid surface are defined by

$$\tau'_\text{w} = a\,\hat{\tau}_\text{w} \exp\{i\,\alpha\,(x - C\,t)\}\ , \tag{2}$$

$$P'_\text{w} = a\,\hat{P}_\text{w} \exp\{i\,\alpha\,(x - C\,t)\}\ , \tag{3}$$

where $\hat{\tau}_\text{w} = \tau_\text{wR} + i\,\tau_\text{wI}$ and $\hat{P}_\text{w} = P_\text{wR} + i\,P_\text{wI}$ are complex quantities. Hence, if only the real parts of (2) and (3) are considered, we get

$$\tau'_\text{w} = a \exp(\alpha\,C_\text{I}\,t)\,[\tau_\text{wR} \cos\alpha(x - C_\text{R}\,t) - \tau_\text{wI} \sin\alpha(x - C_\text{R}\,t)]\ , \tag{4}$$

$$P'_\text{w} = a \exp(\alpha\,C_\text{I}\,t)\,[P_\text{wR} \cos\alpha(x - C_\text{R}\,t) - P_\text{wI} \sin\alpha(x - C_\text{R}\,t)]\ . \tag{5}$$

If the disturbances defined this way are introduced into the equations of motion, the eigenvalue problem for the wave velocity C is obtained. For more details see [4].

2.2. Governing equations

As stated Hanratty in [4], the linear stability analysis outlined in 2.1 leads for relatively thick liquid films, i.e. if $(\alpha\,\bar{h})(\bar{h}\,C_{\mathrm{R}}/\nu_{\mathrm{L}})$ is a large number, and under some other restrictions into the two equation system (6)–(7) in which $\bar{u}_0$ denotes the surface velocity, g the acceleration of gravity and ϱ_{L}, ν_{L} and σ denote liquid density, viscosity and surface tension respectively.

$$
\alpha\,(\bar{u}_0 - C)\,\coth(\alpha\,\bar{h}) - \left.\frac{\mathrm{d}\bar{u}}{\mathrm{d}y}\right|_0 (\bar{u}_0 - C) =
$$

$$
= G + \frac{\mathrm{i}\,\hat{\tau}_{\mathrm{w}}}{\varrho_{\mathrm{L}}} \left[\coth(\alpha\,\bar{h}) - \frac{1}{\alpha\,(\bar{u}_0 - C)} \left.\frac{\mathrm{d}\bar{u}}{\mathrm{d}y}\right|_0 \right] -
$$

$$
- (\alpha\,\bar{h})^{1/2} \left(-\mathrm{i}\,\frac{\bar{h}\,C}{\nu_{\mathrm{L}}} \right) \alpha\,(\bar{u}_0 - C)^2 \left[1 - \coth^2(\alpha\,\bar{h}) \right] +
$$

$$
+ 4\,\mathrm{i}\,\alpha\,\bar{h} \left[\frac{\bar{h}\,(\bar{u}_0 - c)}{\nu_{\mathrm{L}}} \right]^{-1} \alpha\,(\bar{u}_0 - C)^2 \left[\coth(\alpha\,\bar{h}) - \frac{1}{\alpha\,(\bar{u}_0 - C)} \left.\frac{\mathrm{d}\bar{u}}{\mathrm{d}y}\right|_0 \right] ,
$$

$$(6)$$

$$
G = \frac{\hat{P}_{\mathrm{w}}}{\varrho_{\mathrm{L}}} + \frac{\sigma\,\alpha^2}{\varrho_{\mathrm{L}}} + g . \tag{7}
$$

The equations for wave phase velocity C_{R} and growth rate C_{I} are obtained by separately equating the real and imaginary parts of (6), keeping only terms of the highest order in $(\bar{h}\,C_{\mathrm{R}}/\nu_{\mathrm{L}})$ as is stated in [4]. The resulting equations have the forms:

$$
0 = (C_{\mathrm{R}} - \bar{u}_0)^2 + \left.\frac{\mathrm{d}\bar{u}}{\mathrm{d}y}\right|_0 (C_{\mathrm{R}} - \bar{u}_0) \frac{\tanh(\alpha\,\bar{h})}{\alpha} - \left(\frac{P_{\mathrm{wR}}}{\alpha\,\varrho_{\mathrm{L}}} + \frac{\alpha\,\sigma}{\varrho_{\mathrm{L}}} + \frac{q}{\alpha} \right) \tanh(\alpha\,\bar{h}) + \frac{\tau_{\mathrm{wI}}}{\alpha\,\varrho_{\mathrm{L}}} -
$$

$$
- C_{\mathrm{I}}^2 + \frac{\tanh(\alpha\,\bar{h})}{\alpha} \left.\frac{\mathrm{d}\bar{u}}{\mathrm{d}y}\right|_0 \left[\frac{C_{\mathrm{R}} - \bar{u}_0}{(C_{\mathrm{R}} - \bar{u}_0)^2 + C_{\mathrm{I}}^2} - \frac{\tau_{\mathrm{wR}}}{\alpha\,\varrho_{\mathrm{L}}} \frac{C_{\mathrm{I}}}{(C_{\mathrm{R}} - \bar{u}_0)^2 + C_{\mathrm{I}}^2} \right] , \tag{8}
$$

$$
\frac{P_{\mathrm{wI}}}{\varrho_{\mathrm{L}}} + \frac{\tau_{\mathrm{wR}}}{\alpha\,\varrho_{\mathrm{L}}} \left[\alpha\,\coth(\alpha\,\bar{h}) + \frac{C_{\mathrm{R}} - \bar{u}_0}{(C_{\mathrm{R}} - \bar{u}_0)^2 + C_{\mathrm{I}}^2} \left.\frac{\mathrm{d}\bar{u}}{\mathrm{d}y}\right|_0 \right] +
$$

$$
+ \frac{\tau_{\mathrm{wI}}}{\alpha\,\varrho_{\mathrm{L}}} \frac{C_{\mathrm{I}}}{(C_{\mathrm{R}} - \bar{u}_0)^2 + C_{\mathrm{I}}^2} \left.\frac{\mathrm{d}\bar{u}}{\mathrm{d}y}\right|_0 =
$$

$$
= 4\,\alpha^2\,\nu_{\mathrm{L}}\,(C_{\mathrm{R}} - \bar{u}_0)\,\coth(\alpha\,\bar{h}) + 4\,\alpha\,\nu_{\mathrm{L}} \left.\frac{\mathrm{d}\bar{u}}{\mathrm{d}y}\right|_0 + 2\,(C_{\mathrm{R}} - \bar{u}_0)\,C_{\mathrm{I}}\,\alpha\,\coth(\alpha\,\bar{h}) + \tag{9}
$$

$$
+ C_{\mathrm{I}} \left.\frac{\mathrm{d}\bar{u}}{\mathrm{d}y}\right|_0 + \frac{\nu_{\mathrm{L}}^{1/2}\,\alpha^{3/2}(\coth^2(\alpha\,\bar{h}) - 1)\,C_{\mathrm{R}}^{1/2}}{2^{1/2}\,(C_{\mathrm{R}}^2 + C_{\mathrm{I}}^2)^{1/2}} \times
$$

$$
\times \left\{ [(C_{\mathrm{R}} - \bar{u}_0)^2 - C_{\mathrm{I}}^2]\,(\cos\theta - \sin\theta) + (C_{\mathrm{R}} - \bar{u}_0)\,2\,C_{\mathrm{I}}\,(\cos\theta + \sin\theta)] \right\} ,
$$

$$
\theta = \frac{1}{2}\,\tan^{-1}\frac{C_{\mathrm{I}}}{C_{\mathrm{R}}} . \tag{10}
$$

In order to solve the governing equations (8)–(10), the liquid velocity $\bar{u}_0$ and the velocity gradient $\mathrm{d}\bar{u}/\mathrm{d}y|_0$ evaluated at the average location of the interface are necessary to determine. Supposing the linearity of the liquid film velocity profile, the velocity gradient equals to $\bar{u}_0/\bar{h}$ and therefore the shear stress on the interface can be computed by

$$
\tau = \mu_{\mathrm{L}} \left.\frac{\mathrm{d}u}{\mathrm{d}y}\right|_0 \cong \mu_{\mathrm{L}}\,\frac{\bar{u}_0}{\bar{h}} . \tag{11}
$$

According to [2], the mean air velocity profile which obeys the $1/7^{\text{th}}$ power law, see [5], leads to formula

$$\frac{U_{\max}}{u_\tau} = 8.74 \left(\frac{H \, u_\tau}{2 \, \nu_{\mathrm{G}}} \right)^{1/7} \; , \tag{12}$$

where $u_\tau = \sqrt{\tau/\varrho_{\mathrm{G}}}$ is the friction velocity. By substituting (11) into (12) we get the dependence of the liquid surface velocity on the maximum air velocity $U_{\max}$ and channel height H given by

$$\bar{u}_0 = \left(\frac{U_{\max}}{8.74} \right)^{7/4} \left(\frac{2 \, \nu_{\mathrm{G}}}{H} \right)^{1/4} \frac{\bar{h} \, \varrho_{\mathrm{G}}}{\mu_{\mathrm{L}}} \; . \tag{13}$$

2.3. Prediction of gas effects

In order to solve the governing equations, the gas effect on the liquid surface manifested in τ_{w} ($\tau_{\mathrm{wR}}, \tau_{\mathrm{wI}}$) and P_{w} ($P_{\mathrm{wR}}, P_{\mathrm{wI}}$) has to be substituted. Although some models of these quantities are developed in literature in dependence on channel height H, wavenumber α and gas bulk velocity U_{b}, e.g. in [1], [4], [6], we decided to design new simple algebraic models using CFD simulations, because of the complexity or the limited applicability of existing models.

Because of the 'quasi-static' assumption, the gas effect can be computed as the wall shear stress and pressure forces acting on the solid wavy surface induced by turbulent flow. Therefore, we have created a set of two-dimensional geometries representing a rectangular channel with flat upper wall and sinusoidal lower wall as is depicted in Fig. 2. The channel height was set $H/\lambda = 0.6, 0.8, 1.0, 1.2, 1.4$ and the wave steepness ratio λ/α was set in range from 20 to 200 while the wavelength λ has been set as a constant equal to 5 cm. The bulk velocity U_{b} was prescribed in range from 2 to 20 m/s which should sufficiently cover the conditions of considered instabilities occurrence.
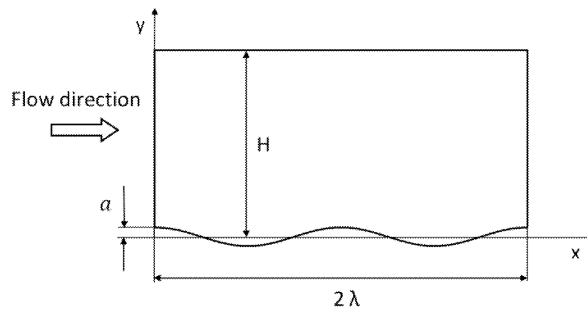

Fig.2: Computational domain for gas effect prediction

Using the results of the set of so defined CFD simulations computed by k-ε V2F turbulence model, the gas effects have been quantified by relations (14)–(17).

$$\tau_{\mathrm{wR}} = 0.214 \, H^{-0.219} \, (\lambda/\alpha)^{-1.080} \, U_{\mathrm{b}}^{1.530}/a \; , \tag{14}$$

$$\tau_{\mathrm{wI}} = 0.070 \, H^{-0.263} \, (\lambda/\alpha)^{-0.920} \, U_{\mathrm{b}}^{1.720}/a \; , \tag{15}$$

$$P_{\mathrm{wR}} = -0.594 \, H^{-0.357} \, (\lambda/\alpha)^{-0.914} \, U_{\mathrm{b}}^{2.240}/a \; , \tag{16}$$

$$P_{\mathrm{wI}} = 21.532 \, H^{-0.124} \, (\lambda/\alpha)^{-1.552} \, U_{\mathrm{b}}^{1.550}/a \; . \tag{17}$$

3. Results and discussion

The solution of governing equations (8)–(10) defines the growth rate $\alpha\,C_I$ depending on wavenumber α, liquid film height h, channel height H, gas velocity U_b and physical constants. Unfortunately, the model is not closed because the specification of the wave amplitude is needed for the gas effects prediction. According to [3], the ratio $a/\bar{h}$ is less than 0.5 for gas Reynolds numbers less than 10^4 and this ratio decreases with decreasing Re_G. Hence, we set $a/\bar{h} = 1/3$ for the instability area determination.

From the dependence of the growth rate $\alpha\,C_I$ on the wavenumber α, see Fig. 3, the wavelength which induced the most growing disturbance can be determined. As can be seen from Fig. 4 and Fig. 5 this wavelength is very close to the experimental observations.

The comparison of maximum growth locus with solution of Frederick [7] computed using model D* of Abrams [6] shows that our model give better prediction of observed conditions
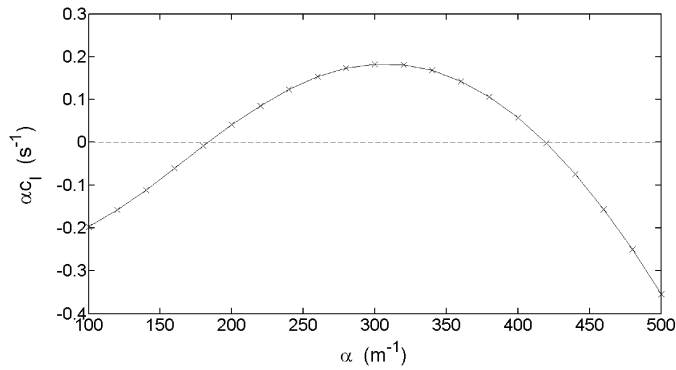
Fig.3: *Dependence of the growth rate $\alpha\,C_I$ on the wavenumber α; geometrical and physical conditions are defined by $H = 25.4\,mm$, $\bar{h} = 4.5\,mm$, $Re_G = 3000$, $\mu_L = 3.9\,mPa\,s$ and $\nu_G = 1.66\times10^{-5}\,m^2 s^{-1}$*
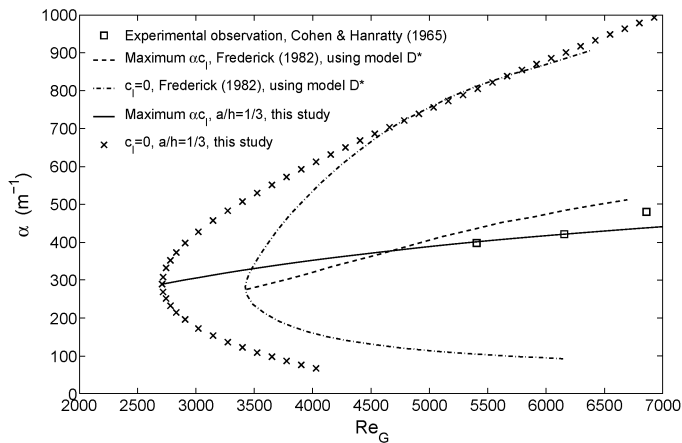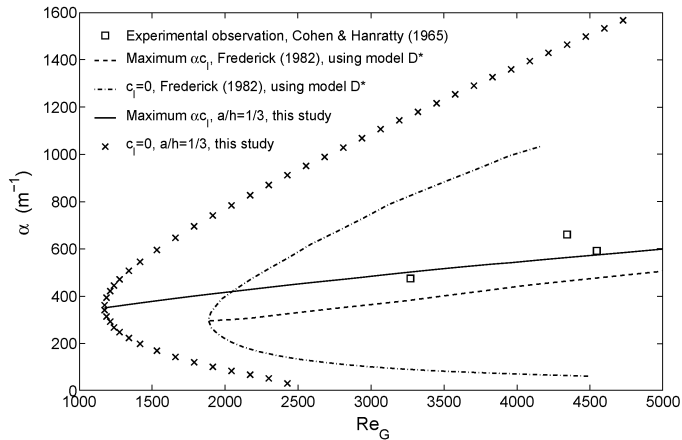

Fig.4: *Comparison of instability area and maximum growth locus with solution of Frederick [7] based on model D* of Abrams [6] and with experimental observations of Cohen & Hanratty [1]; Geometrical and physical conditions are defined by $H = 25.4\,mm$, $\bar{h} = 4.5\,mm$, $\mu_L = 3.9\,mPa\,s$ and $\nu_G = 1.66\times10^{-5}\,m^2 s^{-1}$*

Fig.5: Comparison of instability area and maximum growth locus with solution of Frederick [7] based on model D* of Abrams [6] and with experimental observations of Cohen & Hanratty [1]. Geometrical and physical conditions are defined by $H = 25.4\,mm$, $\bar{h} = 4.9\,mm$, $\mu_L = 0.9\,mPa\,s$ and $\nu_G = 1.60 \times 10^{-5}\,m^2 s^{-1}$
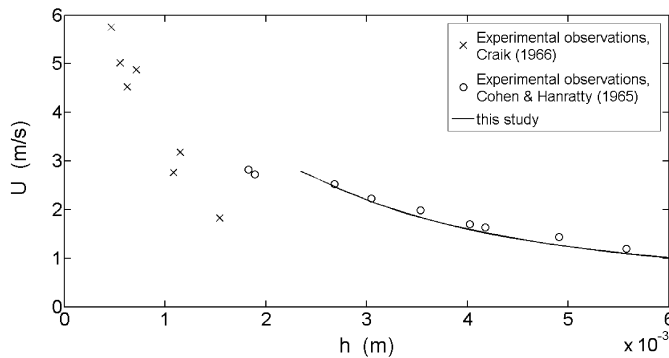

Fig.6: Comparison of this study prediction of transition to two-dimensional waves with experimental data of Cohen & Hanratty in [1] and Craik in [2]; both experiments were carried out in 2.54 high and 30.5 cm wide horizontal enclosed channel

measured by Cohen & Hanratty [1] for both of two different settings described in labels of Fig. 4 and Fig. 5. However, the instability areas defined by $\alpha\,C_I > 0$ are larger and the critical Reynolds numbers (gas velocities) are lower in both cases. This can be explained by the fact that for so low Reynolds numbers when first instability occurs, the wave amplitude must be much lower than $\bar{h}/3$. Very good agreement of the critical gas velocities for different liquid film heights with experimental observations of Cohen & Hanratty [1] was attained for $a/\bar{h} = 1/8$ as is shown in Fig. 6.

Note that the model is applicable only for film thickness larger than about 2.3 mm due to the restrictions of the governing equations mentioned in 2.2. It should by also noted that the measurements of Cohen & Hanratty [1] are slightly inconsistent with transition observed by Craik [2] in Fig. 1 as can be seen from comparison in Fig. 6. The discrepancy is even larger with regard to the fact that in case of Craik the maximum velocities were measured

and not bulk velocities as in case of Cohen & Hanratty. Unfortunately, the reason of this inconsistency is unclear.

The wavelengths corresponding to the critical conditions in Fig. 6 are shown in Fig. 7. The resulting wavelengths ranged from 1.7 to 2.4 cm are quite well consistent with experimental observations of Cohen & Hanratty [1] who state wavelength from 2.2 to 3 cm. However the increase of the wavelengths with decreasing liquid height is in disagreement with observations for thin liquid film ($\bar{h} < 1.6$ mm) of Craik [2] who report wavelengths from 1 to 2 cm. This result supports the conclusion that the prediction of wavelengths is not adequate for liquid film thinner than about 3 mm.
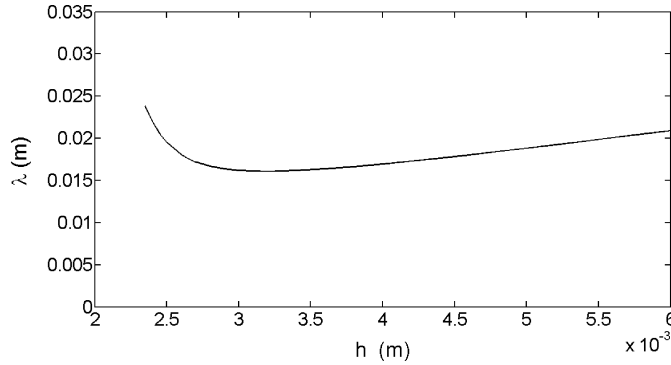

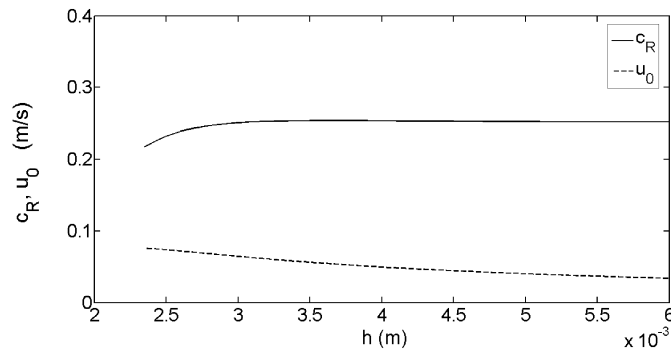Fig.7: *Wavelength corresponding to the critical conditions for instability occurrence*

Fig.8: *Phase velocity and liquid surface velocity corresponding to the critical conditions for instability occurrence*

The phase velocity and liquid surface velocity are depicted in Fig. 8. The phase velocity has the value of about 0.25 m/s while Cohen & Hanratty [1] state the value of about 0.3 m/s. However, our result agrees well with the analytical formula (18), see [8], for phase velocities of surface tension depending gravity waves.

$$c_{\mathrm{R}} = \sqrt{\left(\frac{g\,\lambda}{2\pi} + \frac{2\pi}{\varrho_{\mathrm{L}}\,\lambda} \right) \tanh \frac{2\pi\,H}{\lambda}} \ . \tag{18}$$

The liquid film surface velocities are less than the phase velocities in all cases, which is consistent with experiments, however there is lack of data for more precise comparison.

4. Conclusions

The liquid film stability model based on the linear analysis of momentum equations and gas effects computed using results of CFD simulations is presented. Taking into account the 'quasi-static' assumption, the gas effect on the liquid film has been computed as the wall shear stress and pressure forces acting on the solid wavy surface. Although some models of these quantities are developed in literature, we decided to design new simple formulas, because of the complexity or the limited applicability of existing models. Using the results of the set of properly defined CFD simulations computed by k-ε V2F turbulence model, the gas effects have been quantified by algebraic relations. By substitution of these formulas into the governing equations of motion the desired instability model was closed. Using so defined mathematical model, the critical gas velocity, wavelength and wave phase velocity can be predicted in dependence on average liquid film height $\bar{h}$, channel height H and physical constants. As a consequence of the linearity assumptions, the model is usable for film height thicker than about 2.3 mm. The weakness of the model lies in the fact that the ratio of the wave amplitude to the average liquid film height must be determined. However, using the assumption $a/\bar{h} = 1/3$, the prediction of the maximum growth locus is very good in comparison with experimental observations carried out for two types of geometrical and physical conditions. The precision of the critical gas prediction is depending on the wave amplitude determination. If the ratio $a/\bar{h}$ was set to $1/8$, excellent agreement with experiments of Cohen & Hanratty [1] was achieved. The wavelengths, phase and liquid surface velocities agree well with the experimental observations and analytical formula for gravity waves.

Acknowledgement

References

[1] Cohen L.S., Hanratty T.J.: Generation of waves in the concurrent flow of air and a liquid, A.I.Ch.E. J. 11, pp. 138–144, 1965

[2] Craik A.D.D.: Wind-generated waves in thin liquid films, J. Fluid Mech., vol. 26, part 2, pp. 369–392, 1966

[3] Peng C.-A., Jurman L.A., McCready M.J.: Formation of solitary waves on gas-sheared liquid layers, Int. J. Multiphase Flow, vol. 17, No. 6, pp. 767–782, 1991

[4] Hanratty T.J.: Interfacial instabilities caused by air flow over a thin liquid layers, In R. E. Meyer (Ed.), Waves on Fluid Interfaces, Academic Press, New York, 1983, pp. 221–259

[5] Schlichting H.: Boundary layer theory, New York, McGraw-Hill, 1960, p. 506

[6] Abrams J.: Turbulent flow over small amplitude solid waves, Ph.D. Dissertation, University of Illinois, Urbana, 1983

[7] Frederick K.A.: Wave generation at a gas-liquid interface, M.S. Dissertation, University of Illinois, Urbana, 1982

[8] Kundu P.K., Cohen I.M.: Fluid Mechanics, Fourth Edition, Elsevier, 2008, ISBN 978-0-12373735-9